Curr Cardiovasc Imaging Rep (2014) 7:9309
DOI 10.1007/s12410-014-9309-6

Current Development of Molecular Coronary Plaque Imaging using Magnetic Resonance Imaging towards Clinical Application

Begoña Lavin · Alkystis Phinikaridou · Markus Henningsson · René M. Botnar

Published online: 29 October 2014

Abstract Cardiovascular disease (CVD) remains the leading cause of death in Western countries despite improvements in prevention, diagnosis and treatment. Atherosclerosis is a chronic inflammatory disease that remains clinically silent for many decades. Sudden rupture of "high-risk/vulnerable" plaques has been shown to be responsible for the majority of acute cardiovascular events, including myocardial infarction and stroke. Therefore, early detection of biological processes associated with atherosclerosis progression and plaque instability may improve diagnosis and treatment and help to better monitor the effectiveness of therapeutic interventions. Molecular magnetic resonance imaging (MRI) is a promising tool to detect molecular and cellular changes in the carotid, aortic and coronary vessel wall including endothelial dysfunction, inflammation, vascular remodelling, enzymatic activity, intraplaque haemorrhage and fibrin deposition and thus may allow early detection of unstable lesions and improve the prediction of future coronary events. Evaluation of atherosclerosis at both, the preclinical and clinical level includes non-contrast-enhanced (NCE) and contrast-enhanced (CE) MRI with and without the use of MR contrast agents. To increase the biological information obtained by MRI a variety of targeted-specific molecular probes have been developed for the non-invasive visualization of particular biological processes at the molecular and cellular level. This review will discuss the recent advances in molecular MRI of atherosclerosis, covering both pulse sequence development and also the design of novel contrast agents, for imaging atherosclerotic disease in vivo.

Keywords Molecular MR imaging · Atherosclerosis · Coronary artery disease · Contrast agent

This article is part of the Topical Collection on *Intravascular Imaging*

B. Lavin (✉) · A. Phinikaridou · M. Henningsson · R. M. Botnar
Division of Imaging Sciences and Biomedical Engineering, King's College London, St. Thomas' Hospital, 4th Floor, Lambeth Wing, London SE1 7EH, UK
e-mail: begona.lavin_plaza@kcl.ac.uk

B. Lavin · A. Phinikaridou · M. Henningsson · R. M. Botnar
The British Heart Foundation Centre of Excellence, Cardiovascular Division, King's College London, London, UK

B. Lavin · R. M. Botnar
Wellcome Trust and EPSRC Medical Engineering Center, King's College London, London, UK

Introduction

Cardiovascular disease (CVD) remains the leading cause of death worldwide despite improvements in prevention (e.g. blood pressure control, cholesterol lowering and smoking cessation), and advances in diagnosis and treatment. Coronary artery disease (CAD) and myocardial infarction account for more than 50 % of CVD deaths and are the result of atherosclerosis and plaque rupture with subsequent thrombosis. A major challenge of CAD diagnosis is that 50 % of men and 64 % of women who die suddenly of CVD have no previous symptoms according to the 2013 AHA statistics [1]. The clinical challenge is that the majority of these plaques do not lead to coronary narrowing and/or ischemia but are characterized by outward remodelling and increased biological activity.

Currently used clinical imaging modalities such as x-ray and computed tomography (CT) angiography allow the detection and grading of luminal narrowing. However, they do not provide information on plaque composition and vulnerability [2–4]. Therefore, new non-invasive approaches to detect potentially unstable plaque are urgently needed.

Molecular magnetic resonance imaging (MRI) using target specific imaging agents is an emerging and promising tool to provide more accurate information about plaque composition and biology including endothelial dysfunction, inflammation

and positive remodelling. Molecular MRI thus may improve the prediction of future coronary events, allow earlier and more aggressive medical treatment, monitor the effectiveness of medical and/or interventional treatment in patients and may provide novel data on the pathogenesis of atherosclerosis in vivo.

Pathophysiology of Atherosclerosis

Atherosclerosis is an inflammatory disease that affects medium and large size arteries and usually remains asymptomatic until late stage disease when plaques enlarge and reduce arterial blood flow or suddenly rupture thereby causing thrombotic occlusion and ultimately ischemic events [5, 6] (Fig. 1). It is widely accepted that vascular inflammation is the result of endothelial damage and the subsequent accumulation of low density lipoproteins (LDL) that initiate a complex signalling cascade leading to the recruitment of monocytes and macrophages and the deposition of extracellular matrix (ECM) proteins in the inner layer of the vessel wall [5, 7]. Recent studies have also reported a role of the adventitia [8–10]. Atherosclerosis usually occurs at predilection sites with disturbed laminar flow, such as branch points or at sites with oscillating shear stress [11]. The initial phase is characterized by endothelial dysfunction with structural and molecular alterations, including increasing width of the tight junctions [12, 13] and the activation of cell adhesion molecules, such as intercellular and vascular cell adhesion molecule-1 (ICAM-1 and VCAM-1) and E- and P-selectins [5]. Overexpression of ICAM-1 and VCAM-1 molecules is directly related with an increase in monocyte infiltration in the vessel wall where they differentiate into tissue resident macrophages [14]. Recruitment of immune cells into the artery wall plays a central role in all stages of atherosclerosis. Macrophages uptake oxidized LDL using the scavenger receptors. As a result of continued intra cellular LDL accumulation in macrophages (cytosolic droplets), they transform into foam cells [5, 7]. Subsequent steps include secretion of inflammatory cytokines, activation of platelets, smooth muscle cell proliferation, accumulation of apoptotic cells and deposition of ECM proteins such as collagen and elastin that collectively contribute to the formation of complex plaque including a necrotic lipid core due to foam cell apoptosis at advanced stages [15]. Alteration and

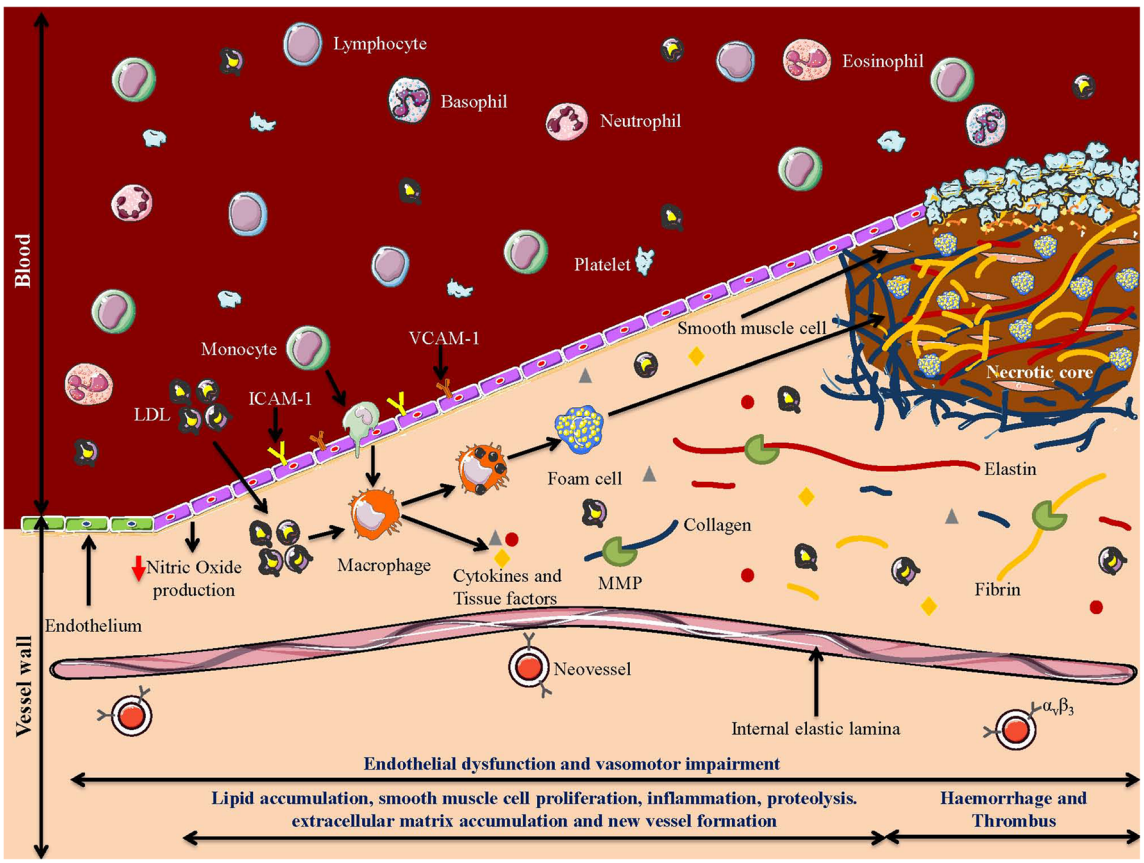

Fig. 1 Pathogenesis of atherosclerotic plaque development. Endothelial dysfunction initiates inflammatory processes and leads to the migration of immune cells and LDL into the vessel wall where monocytes differentiate into macrophages that transform into foam cells with accumulation of lipids and cholesterol. Subsequently, atherosclerotic plaques develop and are characterized by activation of platelets and smooth muscle cells, followed by deposition of extracellular matrix components, endothelial proliferation and necrotic core formation

degradation of the ECM by the release of matrix metalloproteinases (MMPs) from macrophages can lead to the progression and destabilization of the plaque [16•]. Clinically, the aim is to divide atherosclerotic lesions into low risk (stable plaques) and high risk (vulnerable plaques). Post mortem studies have demonstrated that vulnerable plaques are characterized by a large plaque volume and large necrotic core, low amount of fibrous tissue, accumulation of macrophages and a thin fibrous cap. At advanced disease stages, the enlargement of the plaque results in intraplaque hypoxia that triggers additional inflammatory cell infiltration and promotes local neovascularization. Stable plaques are characterized by a thick fibrous cap, high amounts of fibrous tissues and a small number of macrophages [17, 18].

Contrast Agents for Molecular Magnetic Resonance Imaging

Principles

Cardiac MRI has become a clinically accepted imaging modality for myocardial tissue characterization and due to technical advances in MR acquisition and reconstruction and contrast agent development coronary MRI and vessel wall imaging is an emerging non-invasive imaging technique for comprehensive coronary assessment. Compared to other clinical imaging modalities such as single-photon emission computed tomography (SPECT) and position emission tomography computed tomography (PET/CT), MRI provides high spatial and temporal resolution allowing for a comprehensive cardiac evaluation including morphology, function, perfusion and myocardial tissue characterization [19, 20]. The development of novel plaque specific MR contrast agents also allows imaging of biological processes in the vessel wall without exposure of the patient to harmful ionizing radiation.

MRI is based on the nuclear magnetic properties of atoms (mainly hydrogen) and involves the interplay of three components to generate tomographic images: the main magnetic field of the scanner (static magnetic field) which generates a net magnetization along the scanner axis, the gradient fields which are used for spatial localization, and the oscillating magnetic field of the radio frequency (RF) pulses. RF pulses are used to change the orientation of the magnetisation, inducing excitation of the water protons. Following the RF pulse excitation, protons return to their equilibrium stage and specific receiver coils detect the energy emitted during this relaxation. The most important proton properties used by MRI are the proton density and two characteristic relaxation times called spin-lattice relaxation time and spin-spin relaxation time, denoted as T_1 and T_2 respectively. Signal intensity primarily depends on the local values of R_1 ($1/T_1$) and R_2 ($1/T_2$) relaxation rate of water protons [21]. Considering the relatively low sensitivity of MRI, the use of specific contrast agents aid the detection of differences between pathological and normal surrounding tissues. For that, local concentrations of a contrast agent are needed to alter the relaxation rate of water protons sufficiently for detectable signal effects. An important consideration to take into account during vessel wall imaging is the distribution of the contrast agent in non-targeted regions and the adjacent blood pool. In some cases, to distinguish between the luminal area and the vessel wall contrast uptake it might be necessary to wait for the contrast agent to clear sufficiently from the blood.

Technical Considerations

Vessel wall MRI can be achieved without contrast agents by exploiting the ability of MRI to suppress signal from adjacent tissues which mainly include luminal blood and epicardial fat. Fat suppression is commonly performed using spectrally selective inversion magnetization preparation pulses, where the image acquisition is timed to coincide with the nulling point of the fat signal (Fig. 2). Alternatively, signal from fat can be minimized using water selective RF pulses for imaging [22]. To suppress blood signal (so called black-blood MRI), traditionally, flow-dependent techniques have been employed such as double inversion recovery (DIR) [23, 24]. However, DIR is typically limited to two-dimensional cross-sectional imaging of the vessel wall or requires local inversion pulses for three-dimensional coronary vessel wall imaging [25]. More recently, motion-sensitized driven equilibrium (MSDE) [26] and delay altering with nutation for tailored excitation (DANTE) [27] have been proposed to allow for flow-dependent three-dimensional coverage. Such volumetric coverage is desirable due to the long and tortuous geometry of the coronary arteries, and simplifies MRI scan planning compared to DIR. Blood signal suppression can also be achieved using flow-

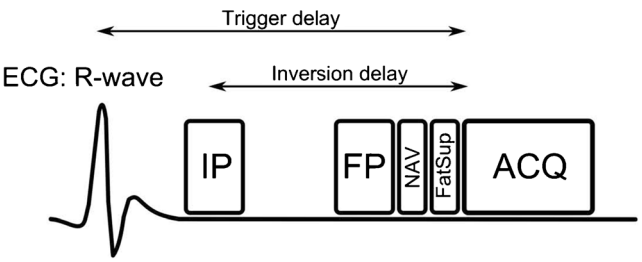

Fig. 2 Generic black-blood vessel wall MRI pulse sequence. Cardiac motion is compensated for by synchronizing the image acquisition (ACQ) with an electrocardiogram (ECG) and using a trigger delay from the R-wave to time ACQ to mid-diastole. Respiratory motion compensation can be performed using respiratory navigation (NAV) which typically precedes ACQ. Fat suppression is performed prior to ACQ using a fat-selective RF pulse to null the fat signal. Black-blood contrast can be achieved either with inversion preparation (IP) where an inversion delay is used to null signal from the blood, or alternatively using flow preparation (FP) where signal from flowing blood is destroyed using de-phasing gradients or a combination of small RF pulses and gradients

independent techniques which typically rely on the difference in T_2 between vessel wall and blood [28] or a combination of T_2 and T_1 [29]. Flow-independence overcomes the problem of inadequate blood suppression in the case of slow laminar flow and facilitates volumetric whole-heart coverage. Vessel wall MRI can also be performed using contrast agents, either with T_1-shortening gadolinium based agents or T_2/T_2* shortening iron based agents, which will be described in detail in following sections.

An important requirement for coronary vessel wall visualization is high spatial resolution. Although sufficient spatial resolution can be achieved with the use of dedicated multi-channel cardiac receiver coils, coronary vessel wall imaging is challenging due to the slow acquisition speed of MRI relative to the physiological motion. This includes both cardiac and respiratory motion, which are both one order of magnitude larger than the achievable spatial resolution. However, to mitigate the effects of motion, which include image blurring and ghosting, cardiac and respiratory motion compensation methods have been introduced. Cardiac motion can be effectively minimized by synchronizing the MRI scanner with an electrocardiogram (ECG) and limit the data acquisition to the most quiescent cardiac phase. Although the timing and duration of the cardiac rest period is subject and heart-rate dependent, time resolved MRI cine scans can be used to identify the most suitable acquisition window. For respiratory motion compensation, a so called respiratory navigator can be used. Conventional respiratory navigator techniques involve measuring the displacement of the lung-liver interface in feet-head direction and only accept data acquired within a narrow 'gating window', typically defined around end-expiration. Furthermore the measured navigator position can be used to update the MRI image in real-time based on a motion model which is often assumed to be a linear relationship of 0.6. A drawback of this approach is that the scan time is prolonged because a large portion of the data falls outside the gating window and has to be re-measured (typically only 20-50 % is inside the window), as well as the indirect motion measurement. Recently, technical advances has allowed for direct measurement of respiratory induced motion using self-gating or image navigators, which directly measure the respiratory motion of the heart which and thus obviate the need for a gating window and reduce scan time [22].

T_1 Contrast Agents

The most commonly used contrast agents are based on gadolinium (Gd) complexes that lead to positive contrast detected as a local increase in MRI signal intensity or brightness [30]. Gd(III) is a metallic element with seven symmetrical, unpaired electrons characterized by a strong paramagnetic susceptibility, which produces a slow electron spin relaxation rate that significantly affects the surrounding water protons. Therefore, it has the effect of shortening T_1 relaxation time in tissues where it accumulates, enhancing the signal in post-contrast T_1-weighted images. Following Gd(III) administration, they rapidly distribute into the extracellular fluid space. Subsequently, they are then gradually excreted via the kidneys with a 60-90 min half-life for most small molecular weight agents (~1000 Da) in patients with normal renal function and completely eliminated after 24 h [30]. Due to its toxicity Gd(III) must be chelated for in vivo application. Several chelating approaches have been published with cyclic chelates (DOTA) demonstrating better metabolic stability than linear chelates (DTPA) [31]. Another important aspect is the optimization of the relaxivity properties of these Gd(III) complexes to improve signal enhancement and therefore the sensitivity of these imaging agents. For protein or cell specific imaging targeting moieties have been attached to Gd(III)-chelates to allow the evaluation of molecular or cellular changes associated with different disease stages. The relaxivity of gadolinium chelates is dependent on several parameters such as, molecular motion and water exchange [30]. A good example of the impact of these two parameters on relaxivity is the Gd-DTPA analog Gadofosveset trisodium, Ablavar (Lantheus Medical Imaging, North Billerica, USA) which binds to human serum albumin and increases its relaxivity by fivefold compared to the unbound fraction [32]. This effect is known as receptor-induced magnetization enhancement (RIME) [33] and has been exploited for other protein binding imaging agents including the elastin-binding contrast agent (ESMA) [34] or a fibrin binding contrast agent, EP-2104R [35•]. Other approaches to improve r_1 relaxivity is the use of lipid-perfluorocarbon emulsions that allow increasing the number of Gd(III) atoms per probe. A good example of these lipid-perfluorocarbon emulsions is a fibrin specific contrast agent where multiple Gd(III) atoms were targeted with biotin that can bind to avidin derivatized with an antibody to recognize fibrin (present in the clot) [36]. Another approach is the use of a lipid tail to increase the number of Gd(III) per molecule. A contrast agent that detects angiogenesis by $\alpha_v\beta_3$-targeting is an example of this design [37].

T_2 and T_2* Contrast Agents

Although Gd(III) based contrast agents usually increase $1/T_1$ and $1/T_2$ (R_1 and R_2, respectively) in similar amounts [38–40], it is well established that iron particle-based contrast agents

have a much stronger effect on increasing R_2 [41]. The paramagnetic properties of iron particles usually disturb the surrounding magnetic field causing a negative contrast effect detected as a decrease of signal intensity or darkness. This effect can be accurately detected with T_2- and T_2*-weighted imaging sequences. Moreover, it has also been demonstrated that iron-based particles can provide higher sensitivity in target detection compared to gadolinium-based contrast agents [42]. Depending on the size range of these particles they can be divided in: micron-sized iron oxide particles (MPIO)≈10 μm in diameter, monocrystalline iron oxide particles (MION)≈3 nm in diameter, ultrasmall superparamagnetic iron oxide particles (USPIO)≈15-30 nm and superparamagnetic particles iron oxide particles (SPIO)≈ 60-180 nm. SPIOs have an iron oxide core that is stabilized with a monomer- or polymer-coating. SPIOs are characterized by good suspensibility, uniform particle size distribution, highly reactive surface and the possibility of coating modifications to attach specific ligands for biomedical applications. The size and surface properties (in particular charge) have a decisive influence on the elimination, cell response and toxicity. The maximum effect of SPIO in tissue is usually detected 24-48 hours after administration [43]. The non-specific uptake of SPIOs by the mononuclear phagocyte system after intravenous administration is well stablished. This process allows the use of SPIOs in both to image organs, in particular, the liver, spleen, lymph nodes and bone marrow [44]. One of the major drawbacks of iron-containing particles due to the non-specific uptake by mononuclear phagocytes is the short blood half-life that limits their application in MRI. In order to increase the blood half-life of these particles, several approaches have been implemented, of which modifying the probe-coating and decreasing their hydrodynamic diameter (e.g. USPIO) are the most frequent. USPIOs are iron oxide nanoparticles composed of $Fe2O_3$ and $Fe3O_4$ stabilized by different coating agents. USPIOs are predominantly used for molecular imaging of atherosclerosis [45], myocardial infarction [46] and cancer [47]. Various studies have demonstrated the possibility to identify carotid plaque inflammation non-invasively using USPIOs in both, animals and human [48–51]. The use of USPIO particles has allowed the direct visualization of macrophage infiltration in carotid atheroma in vivo [52]. Additionally, USPIOs have a high r_1, which produces an increase in signal intensity using T_1-weighted sequences. At low USPIO concentrations, a T_1-enhancing effect can be observed, whereas at higher doses, the susceptibility phenomenon balances the T_1 effect (nonlinearity in the signal-concentration relationship). Thus, according to the sequence and the local concentration of USPIO, T_1, T_2, and T_2* enhancing effects can be observed independently. In this regard, USPIOs can also be used for T_1-weighted imaging to acquire angiograms of the coronary arteries, carotid arteries and aorta.

Contrast Agents

Endothelial Dysfunction

During the first stages of atherosclerosis, the endothelium develops several functional alterations due to cardiovascular risk factors such as smoking, diabetes, hypercholesterolemia and obesity, a condition known as endothelial dysfunction [12]. Under these circumstances, endothelial cells are characterized by a reduction in the net production of nitric oxide (NO), leading to impaired vasodilation and an increase in endothelial permeability that allows the influx of LDL and inflammatory cells into the vessel wall [5]. Additionally, endothelial cells increase the expression of surface specific adhesion molecules such as VCAM-1, ICAM-1 and E- and P-selectins that contribute to the adhesion and infiltration of immune cells into the vessel wall [5]. Several studies have observed a correlation between endothelial dysfunction and plaque burden, representing an interesting imaging target [53]. Gadofosveset is a clinically approved contrast agent with a long blood half-life time due to binding to human serum albumin and thus ideally suited for MR angiography [32, 40]. Recent studies by our group have demonstrated the ability of gadofosveset to detect changes in endothelial permeability in the brachiocephalic artery of atherosclerotic ApoE-/- mice [54•] (Fig. 3) and for monitoring effectiveness of interventions in retarding plaque progression [55]. Gadofosveset enhancement has also been correlated with leaky neovessels in atherosclerotic rabbits [56], stent-induced coronary injury in swine [57] and patients with carotid artery disease [58]. Endothelial adhesion molecules are highly expressed in the early stages of atherosclerosis and therefore different approaches have been developed to specifically image those molecules. In vivo imaging of atherosclerotic plaque has been successfully performed in ApoE-/- mice using VCAM-1-specific nanoparticles [59, 60].

Hypoxia: Angiogenesis and Apoptosis

During the progression of atherosclerosis, the size and composition of the vessel wall changes and local hypoxic areas can contribute to the generation of new vessels, a process known as angiogenesis [61]. This process plays a central role in plaque enlargement and disease progression and the density of neovessels has been linked with vulnerable or unstable plaques [62]. Gadofosveset has been successfully used to image neovessel rich-areas in different animal models and patients [58, 63, 64]. In contrast to healthy tissues, endothelial cells of immature neovessels are activated and express the surface marker $\alpha_v\beta_3$ in significant amounts [65, 66]. It has

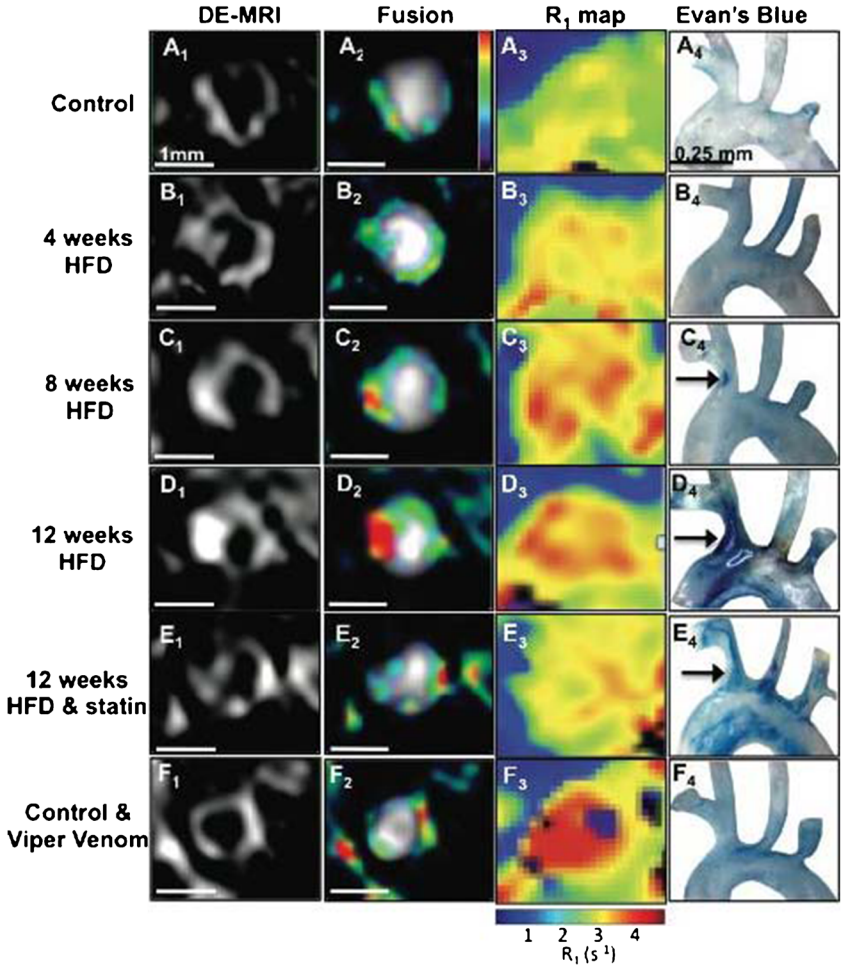

Fig. 3 Uptake of gadofosveset correlates with endothelial permeability and plaque progression. (**A1** through **F1**) and (**A2** through **F2**), Cross-sectional delayed-enhancement magnetic resonance imaging (DE-MRI) and DE-MRI fused with magnetic resonance angiography images of the brachiocephalic artery. Apolipoprotein E–deficient mice on a high-fat diet (HFD) show a gradual increase of vessel wall enhancement corresponding to plaque progression, whereas statin-treated apolipoprotein E–deficient mice show less enhancement. Wild-type mice injected with Russell's viper venom also show increase enhancement compared with non-injected WT mice. (**A3** through **F3**), Corresponding relaxation rate (R1) maps quantify the amount of gadofosveset within the vessel wall. Intense yellow signal indicates increased gadofosveset concentration. (**A4** through **F4**), In situ Evans blue staining shows increased endothelial leakage in regions of DE-MRI with the use of gadofosveset. N=8 per group for the MRI experiments and n=3 per group for the Evans blue dye staining. Adapted from [54•]

been demonstrated that $\alpha_v\beta_3$ targeted paramagnetic nanoparticles allow the non-invasive assessment of $\alpha_v\beta_3$-integrin expression in the aortic wall of hyperlipidemic rabbits during the first stages of atherosclerosis [37]. Alternative approaches include the use of dynamic contrast enhanced T_1-weighted MR imaging using clinically approved contrast agents such as gadopentetate dimeglumine [67].

Hypoxic conditions can also lead to the apoptosis of immune cells which has been described as another marker of plaque instability [68]. During apoptosis, cells express specific surface markers like Annexin-5 or caspases [69]. An Annexin A5-functionalized micellar contrast agent has been successfully used to image apoptosis in atherosclerotic ApoE-/- mice [70]. Moreover, a novel caspase-3/7-activatable Gd-based probe (C-SNAM) has been successfully used to image apoptosis in experimental mouse tumour models [71].

Macrophages

During the progression of atherosclerosis there is a constant influx of immune cells into the vessel wall. The most prominent immune cells that invade these lesions are monocytes that differentiate into plaque resident macrophages where they uptake large amounts of cholesterol to generate so-called foam cells filled with numerous cholesterol ester droplets [5]. Macrophages can alter their phenotype and function in response to the local microenvironment also known as macrophage polarization [72]. In this regard, there is evidence

suggesting that different stages of atherosclerosis are associated with distinct macrophage subtypes, M1, classically-activated or pro-inflammatory macrophages and M2, alternatively-activated or resolving macrophages [72]. Although different strategies have been developed to target monocytes, none of them has had the ability to distinguish between macrophage subtypes. Thus, the development of an M1 or M2 specific probe remains an interesting challenge. The phagocytic properties of macrophages have been used for the passive targeting using different types of iron particles in both, animal models [50, 73–78] and humans [51, 79–81] (Fig. 4). An alternative to non-specific nanoparticles are receptor specific probes. The scavenger receptors are macrophage specific surface proteins that are significantly overexpressed on activated macrophages and foam cells, but not expressed on other cells [49]. With the use of gadolinium immunomicelles targeted to the macrophage scavenger receptor CD206 activated macrophages have been successfully imaged in atherosclerotic plaque of ApoE-/- mice [49]. An alternative approach for macrophage imaging has been developed using gadolinium-loaded LDL-based nanoparticles and modified HDL nanoparticles. Fluorine-containing nanoparticles are avidly taken up by macrophages and therefore can be used to quantify the recruitment of inflammatory cells into atherosclerotic lesions. Since fluorine is absent in the human body, the measurement of fluorine uptake offers a unique possibility to directly detect and quantify the temporal and spatial evolution of the inflammatory response. In vivo imaging of cardiac and cerebral ischemia has been successfully performed in mice using this approach [82] (Fig. 5).

Lipids

Uptake of lipids into the vessel wall is one of the processes present throughout the development of atherosclerosis [5, 72]. There is a strong relationship between high serum lipid levels, especially of low-density lipoproteins (LDL), and coronary

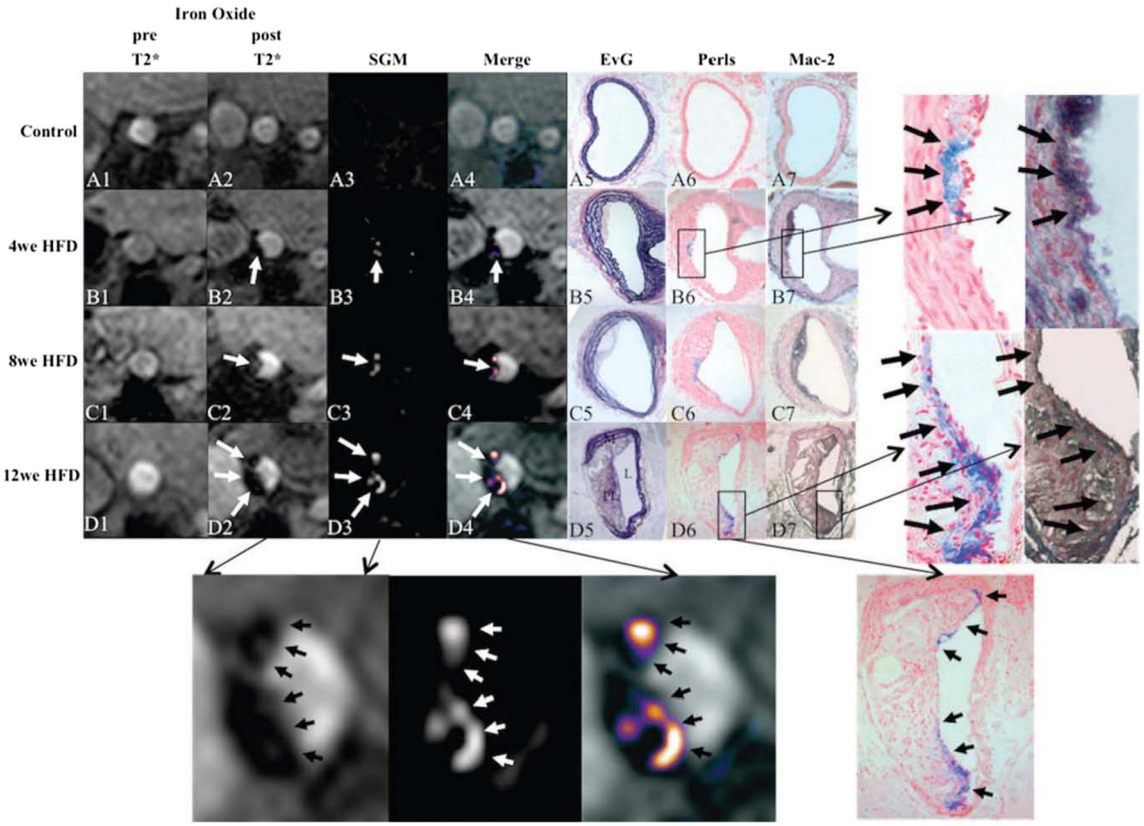

Fig. 4 In vivo imaging of the brachiocephalic artery in ApoE-/- mice on an HFD. Bright-blood imaging was performed such that a 2D slice was obtained perpendicular through the brachiocephalic artery (**A1**–**2**, **B1**–**2**, **C1**–**2** and **D1**–**2**). SGM-positive contrast images were derived and merged with the bright-blood images (**A3**–**4**, **B3**–**4**, **C3**–**4** and **D3**–**4**). Representative images after the injection of the iron oxide agent from control as well as mice on the HFD for 4, 8 and 12 weeks and corresponding elastica–van Giesson stain, Perls stain, and immunohistochemical analysis for Mac-2 (macrophage marker). Contiguous histological sections were taken in a similar orientation as the in vivo MRI of the brachiocephalic artery. Perls staining was used to demonstrate colocalization of iron-positive areas (**A6**, **B6**, **C6** and **D6**) with Mac-2-positive (**A7**, **B7**, **C7** and **D7**) (M indicates media; Pl, plaque; and L, lumen). Adapted from [78]

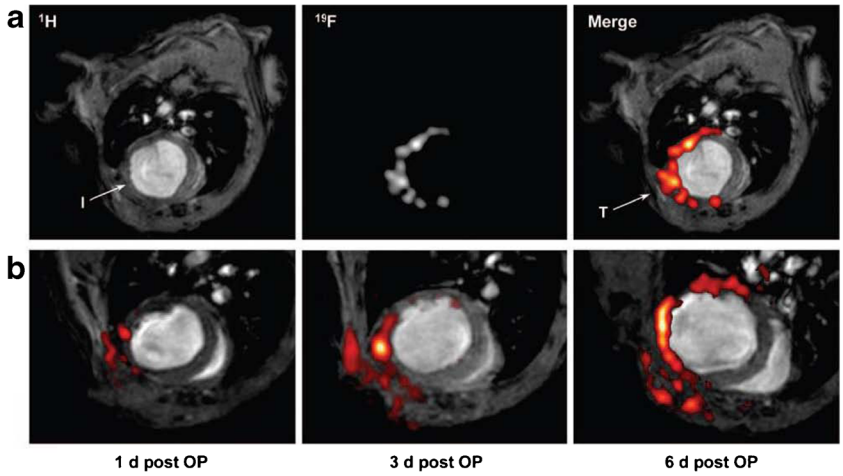

Fig. 5 Infiltration of perfluorocarbons (PFCs) after myocardial infarction as detected by in vivo 19 F MRI. A, Anatomically corresponding 1H and 19 F images from the mouse thorax recorded 4 days after ligation of the LAD showing accumulation of 19 F signal near the infarcted region (I) and at the location of surgery where the thorax was opened (T). PFCs were injected at day 0 (2 hours after infarction) via the tail vein. B, Sections of 1H images superimposed with the matching 19 F images (red) acquired 1, 3, and 6 days after surgery (post OP) indicate a time-dependent infiltration of PFCs into injured areas of the heart and the adjacent region of the chest affected by thoracotomy. Note that at day 4, an additional bolus of PFCs had been injected to compensate for clearance of the particles from the bloodstream after 3 days. Adapted from [82]

risk [83]. Since oxidized LDL is one of the drivers of vessel wall inflammation it represents an interesting imaging target. Gadofluorine M is a gadolinium-based contrast agent that has been successfully used to image increased neovascularization in advanced lipid-rich atherosclerotic lesions in rabbits [84]. Moreover, the incorporation of an ApoE-derived lipopeptide (P2fA2) into the lipid layer of HDL nanoparticles (rHDL–P2A2) has been developed as a platform for molecular MRI of macrophages in atherosclerotic plaques in vivo [85].

Extracellular Plaque Components and Proteolytic Enzymes

Another approach to non-invasive image atherosclerosis is targeting extracellular plaque components. The extracellular matrix is a protein and carbohydrate based lattice. In atherosclerotic vessels, smooth muscle cells and macrophages increase the synthesis and secretion of ECM components such as collagen and elastin and this turnover is related with vascular wall remodelling [86]. To detect the alteration of the ECM under pathological conditions a small molecular weight elastin specific gadolinium based contrast agent (ESMA) has been developed. The ability of ESMA to detect plaque burden and ECM remodelling has been demonstrated at different stages of atherosclerosis in a murine model and in a porcine model of coronary injury [34, 87, 88] (Fig. 6). In addition to quantifying the plaque burden using the ESMA, a study using a rabbit model of experimentally induced thrombosis allowed in vivo classification of vascular remodelling in negative, intermediate, and positive for the detection of "high risk/vulnerable" plaque [89•] (Fig. 7). Similarto prospective clinical studies in humans with coronary artery disease [17, 90, 91], the rabbit study showed that positive remodelling measured after administration of ESMA was associated with plaque instability.

An alternative to directly imaging the ECM is to target proteolytic enzymes that are implicated in the degradation of ECM components such as collagen and elastin [86, 92]. These enzymes are mainly secreted by macrophages and are known as matrix metalloproteinases or MMPs. MMPs have been linked to plaque instability [92]. Noninvasive imaging of MMPs has been successfully performed using a gadolinium chelate targeted to a MMP inhibitor (P947) in murine and rabbit experimental models [93, 94]. Moreover, the enzyme myeloperoxidase (MPO) has been used as an emerging biomarker of plaque instability and future acute events [95]. The feasibility of a specific gadolinium-based probe that targets MPO-Gd to image atherosclerosis in hyperlipidemic rabbits has also been demonstrated [96]. In addition, MPO-Gd enhancement colocalizes with plaque areas rich in infiltrated macrophages [97].

Fibrin and Thrombus Formation

Fibrin plays a central role in thrombus formation but it has also been identified in atherosclerotic lesions of the aorta and coronary arteries [98]. Fibrin I and II are present in several types of atherosclerotic plaque, with fibrin II predominating in later stages and usually colocalizes with macrophages [98]. Although fibrin may enter the intima after mural thrombi originating from plaque rupture or erosion, fragile newly formed vessels may also provide a site of entry [99]. Different fibrin-specific contrast agents have been evaluated in different

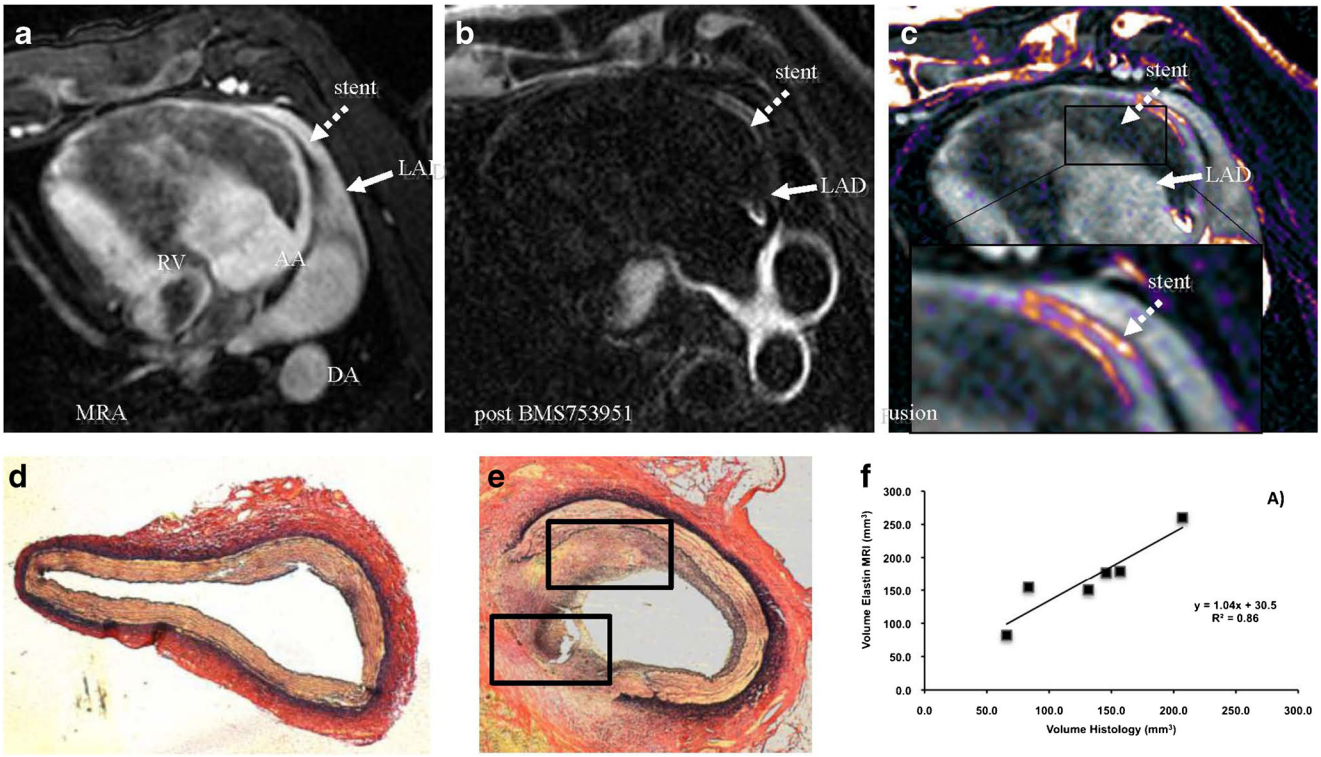

Fig. 6 Elastin imaging of coronary remodelling. Comparison of coronary MRA (**a**), delayed-enhancement MRI (**b**), and positron-emission CT–like fusion of A and B (**c**) of stented and control coronary vessel segments and corresponding histology (**d** and **e**). Strong enhancement can be observed at the stent location (dotted white arrow), whereas little to no enhancement is visible in the normal noninjured left anterior descending artery segment (**b** and **c**). Elastic von Gieson stain of noninjured coronary vessel segment (**d**) shows intact internal elastic lamina (IEL) and circular arranged elastin fibers (black) in the media. Elastic von Gieson of stented vessel segment (**e**) demonstrates disruption of IEL and neointima formation with diffuse elastin deposition (black dots). (**f**) Scatterplot showing correlation between volume of enhancement after administration of BMS-753951 and volume of combined intima+media by histology. Adapted from [87]

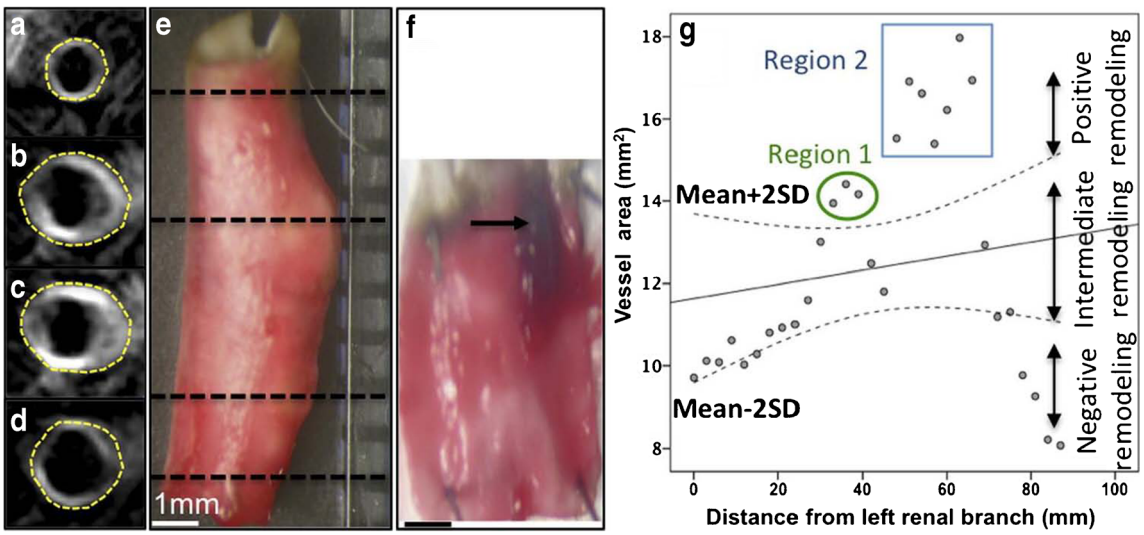

Fig. 7 Positive vascular remodelling in disrupted plaques. (**a**–**d**), DE MR images obtained after administration of elastin-specific contrast agent show positive remodelling, as defined by enlargement of vessel area (yellow contours). (**e**), Corresponding *en face* photograph verifies presence of positive vascular remodelling. (**f**), *En face* photograph of longitudinally open vessel shows thrombus (arrow) attached to vessel wall at proximal end of positive remodelling. (**g**), Scatterplot shows change in vessel area measured on consecutive slices along aorta, starting from left renal branch (0 mm) to iliac bifurcation (86 mm). Two regions of the vessel wall underwent positive remodelling, with vessel areas falling above the mean +2 SD margin. Both plaques disrupted after triggering. Four of seven sections covering the vulnerable region 2 are illustrated in (**a**–**d**). Adapted from [89•]

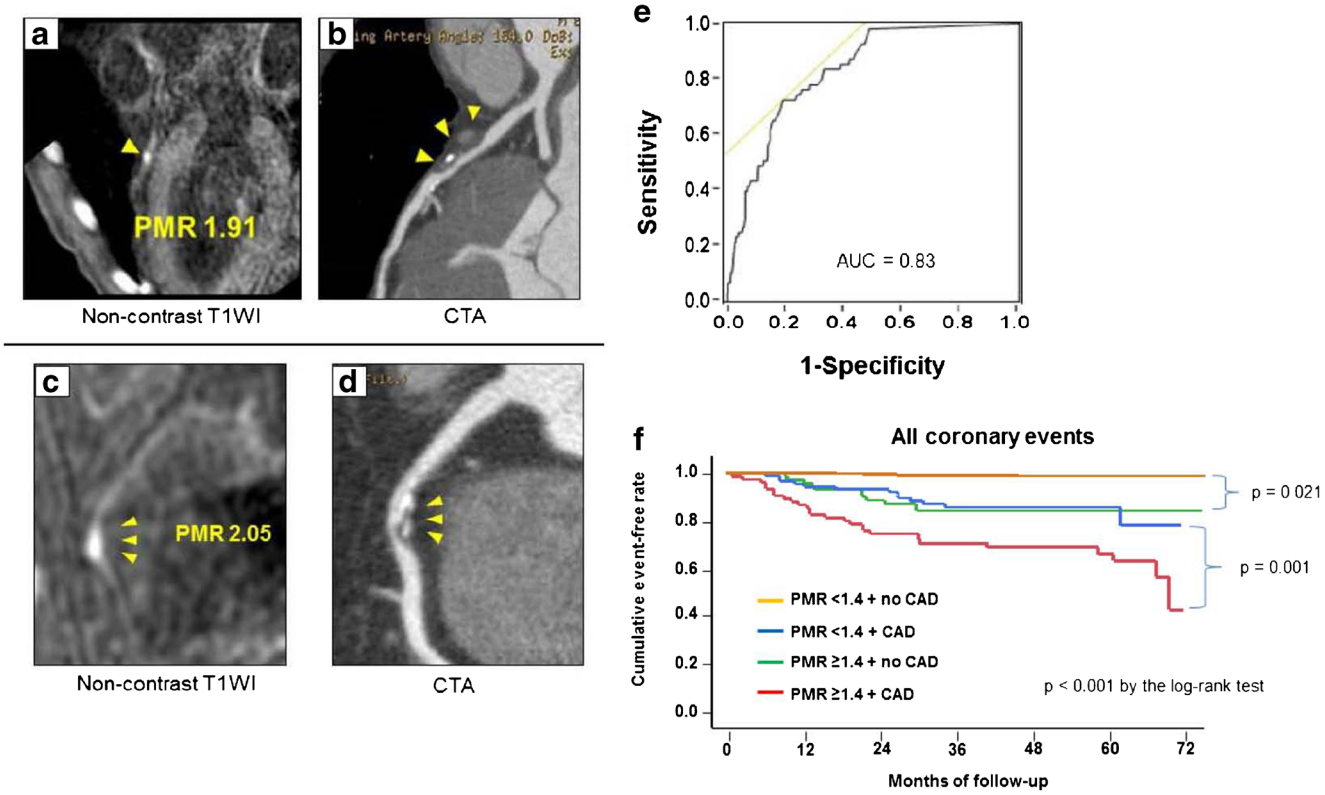

Fig. 8 Representative Images of HIPs with PMRs ≥1.4. Representative noncontrast T1-weighted images of high-intensity plaques (HIPs) (**yellow arrowheads**) in the proximal left anterior descending coronary artery (**a**) and the right coronary artery (**c**), in which plaque-to-myocardium signal intensity ratios (PMRs) were 1.91 and 2.05, respectively. These high-intensity signals each correspond to the left and right coronary plaques on computed tomographic angiography (CTA) (**yellow arrowheads** on curved multiplanar reformation images, **b** and **d**). T1WI=T1-weighted imaging. (**e**) ROC curve analysis for developing coronary events and flowchart of study patients on the basis of PMR. From receiver-operating characteristic (ROC) curve analysis, a plaque-to-myocardium signal intensity ratio (PMR) of 1.4 was identified as the best cutoff value for predicting cardiac events, with 69.5 % sensitivity and 82.3 % specificity. The calculated area under the curve (AUC) was 0.83. (**f**) Kaplan-Meier curves comparing the probability of all coronary events. Coronary event–free survival was worst in the group with plaque-to-myocardium. signal intensity ratios (PMRs) ≥1.4 and coronary artery disease (CAD) (**red line**) and best in the group with PMRs <1.4 but no CAD group (**orange line**). The rate in the group with PMRs ≥1.4 and no CAD (**green line**) was intermediate but comparable with that in the group with PMRs <1.4 and CAD (**blue line**) [103••]

vascular beds. Gadolinium-based nanoparticles and small peptides (EP-2104R) targeted to fibrin have been successfully used to image atherosclerosis in both, animal models and humans [35•, 100–102]. The ability of EP-2104R to detect coronary thrombosis has been first demonstrated in a swine model of intra stent thrombus and has been subsequently successfully translated in a small clinically feasible study of aortic and carotid thrombosis [103••] (Fig. 8).

Conclusions

Molecular MR imaging is a promising approach to evaluate biological processes involved in coronary artery disease. This methodology has been successfully validated to image cellular and structural changes in the vessel wall during atherosclerosis progression in animal models and humans. Coronary vessel wall NCE-MR and CE-MR in patients after myocardial infarction has shown potential for the non-invasive characterization of coronary artery plaque (e.g. endothelial dysfunction, haemorrhage and fibrosis) without the use of ionizing radiation. For additional characterization of atherosclerotic lesions, target-specific imaging probes have been developed, which allowed successful imaging of extracellular matrix remodelling and coronary thrombosis. In the future, visualization of both early and late biological changes of coronary lesions may allow a more accurate assessment of disease burden and monitoring of the effectiveness of interventions.

Acknowledgments The authors acknowledge financial support from: (1) the British Heart Foundation (RG/12/1/29262), (2) the Centre of Excellence in Medical Engineering funded by the Wellcome Trust and EPSRC (WT 088641/Z/09/Z) and (3) the Department of Health via the National Institute for Health Research (NIHR) comprehensive

Biomedical Research Centre award to Guy's & St Thomas' NHS Foundation Trust in partnership with King's College London and King's College Hospital NHS Foundation Trust. The views expressed are those of the authors and not necessarily those of the NHS, the NIHR or the Department of Health.

Compliance with Ethics Guidelines

Conflict of Interest Begoña Lavin, Alkystis Phinikaridou, Markus Henningsson, and René M. Botnar declare that they have no conflict of interest.

Human and Animal Rights and Informed Consent This article does not contain any studies with human or animal subjects performed by any of the authors.

References

Papers of particular interest, published recently, have been highlighted as:

- • Of importance
- •• Of major importance

1. Go AS et al. Heart disease and stroke statistics–2013 update: a report from the American Heart Association. Circulation. 2013;127:e6–e245. doi:10.1161/CIR.0b013e31828124ad.
2. Ambrose JA et al. Angiographic progression of coronary artery disease and the development of myocardial infarction. J Am Coll Cardiol. 1988;12:56–62.
3. Varnava AM, Mills PG, Davies MJ. Relationship between coronary artery remodeling and plaque vulnerability. Circulation. 2002;105:939–43.
4. Glagov S, Weisenberg E, Zarins CK, Stankunavicius R, Kolettis GJ. Compensatory enlargement of human atherosclerotic coronary arteries. N Engl J Med. 1987;316:1371–5. doi:10.1056/NEJM198705283162204.
5. Libby P, Ridker PM, Hansson GK. Progress and challenges in translating the biology of atherosclerosis. Nature. 2011;473:317–25. doi:10.1038/nature10146.
6. Sato Y, Hatakeyama K, Marutsuka K, Asada Y. Incidence of asymptomatic coronary thrombosis and plaque disruption: comparison of non-cardiac and cardiac deaths among autopsy cases. Thromb Res. 2009;124:19–23. doi:10.1016/j.thromres.2008.08.026.
7. Choudhury RP, Fuster V, Fayad ZA. Molecular, cellular and functional imaging of atherothrombosis. Nat Rev Drug Discov. 2004;3:913–25. doi:10.1038/nrd1548.
8. Wilcox JN, Waksman R, King SB, Scott NA. The role of the adventitia in the arterial response to angioplasty: the effect of intravascular radiation. Int J Radiat Oncol Biol Phys. 1996;36:789–96.
9. Shi Y et al. Adventitial myofibroblasts contribute to neointimal formation in injured porcine coronary arteries. Circulation. 1996;94:1655–64.
10. Zhao L et al. The 5-lipoxygenase pathway promotes pathogenesis of hyperlipidemia-dependent aortic aneurysm. Nat Med. 2004;10:966–73. doi:10.1038/nm1099.
11. Chiu JJ, Chien S. Effects of disturbed flow on vascular endothelium: pathophysiological basis and clinical perspectives. Physiol Rev. 2011;91:327–87. doi:10.1152/physrev.00047.2009.
12. Cines DB et al. Endothelial cells in physiology and in the pathophysiology of vascular disorders. Blood. 1998;91:3527–61.
13. Brodsky SV, Goligorsky MS. Endothelium under stress: local and systemic messages. Semin Nephrol. 2012;32:192–8. doi:10.1016/j.semnephrol.2012.02.005.
14. Galkina E, Ley K. Vascular adhesion molecules in atherosclerosis. Arterioscler Thromb Vasc Biol. 2007;27:2292–301. doi:10.1161/ATVBAHA.107.149179.
15. Weber C, Noels H. Atherosclerosis: current pathogenesis and therapeutic options. Nat Med. 2011;17:1410–22. doi:10.1038/nm.2538.
16. • Silvestre-Roig C et al. Atherosclerotic plaque destabilization: mechanisms, models, and therapeutic strategies. Circ Res. 2014;114:214–26. *This review stimulates translation of the current knowledge of molecular mechanisms of plaque destabilization into clinical studies. It also summarizes available animal models of plaque destabilization.*
17. Stone GW et al. A prospective natural-history study of coronary atherosclerosis. N Engl J Med. 2011;364:226–35. doi:10.1056/NEJMoa1002358.
18. Narula J et al. Arithmetic of vulnerable plaques for noninvasive imaging. Nature Clin Pract Cardiovasc Med. 2008;5 Suppl 2:S2–10. doi:10.1038/ncpcardio1247.
19. Johnson GA et al. Histology by magnetic resonance microscopy. Magn Reson Q. 1993;9:1–30.
20. Leiner T et al. Magnetic resonance imaging of atherosclerosis. Eur Radiol. 2005;15:1087–99. doi:10.1007/s00330-005-2646-8.
21. Nitz WR. MR imaging: acronyms and clinical applications. Eur Radiol. 1999;9:979–97. doi:10.1007/s003300050780.
22. Keegan J, Gatehouse PD, Yang GZ, Firmin DN. Non-model-based correction of respiratory motion using beat-to-beat 3D spiral fat-selective imaging. J Magn Resonance Imaging JMRI. 2007;26:624–9. doi:10.1002/jmri.20941.
23. Fayad ZA et al. Noninvasive in vivo human coronary artery lumen and wall imaging using black-blood magnetic resonance imaging. Circulation. 2000;102:506–10.
24. Botnar RM et al. Noninvasive coronary vessel wall and plaque imaging with magnetic resonance imaging. Circulation. 2000;102:2582–7.
25. Botnar RM et al. 3D coronary vessel wall imaging utilizing a local inversion technique with spiral image acquisition. Magn Reson Med : Off J Soc Magn Reson Med / Soc Magn Reson Med. 2001;46:848–54.
26. Wang J et al. Improved suppression of plaque-mimicking artifacts in black-blood carotid atherosclerosis imaging using a multislice motion-sensitized driven-equilibrium (MSDE) turbo spin-echo (TSE) sequence. Magn Reson Med Off J Soc iMagn Reson Med / Soc Magn Reson Med. 2007;58:973–81. doi:10.1002/mrm.21385.
27. Li L et al. Black-Blood Multicontrast Imaging of Carotid Arteries with DANTE-prepared 2D and 3D MR Imaging. Radiology.2014;131717. doi:10.1148/radiol.14131717.
28. Andia ME et al. Flow-independent 3D whole-heart vessel wall imaging using an interleaved T_2-preparation acquisition. Magn Reson Med: Off J Soc Magn Reson Med / Soc of Magn Reson Med. 2013;69:150–7. doi:10.1002/mrm.24231.
29. Liu CY, Bley TA, Wieben O, Brittain JH, Reeder SB. Flow-independent T(2)-prepared inversion recovery black-blood MR imaging. J Magn Reson Imaging JMRI. 2010;31:248–54. doi:10.1002/jmri.21986.
30. Caravan P. Strategies for increasing the sensitivity of gadolinium based MRI contrast agents. Chem Soc Rev. 2006;35:512–23. doi:10.1039/b510982p.
31. Calcagno C et al. Gadolinium-Based Contrast Agents for Vessel Wall Magnetic Resonance Imaging (MRI) of Atherosclerosis. Curr Cardiovasc Imaging Repo. 2013;6:11–24. doi:10.1007/s12410-012-9177-x.

32. Caravan P et al. The interaction of MS-325 with human serum albumin and its effect on proton relaxation rates. J Am Chem Soc. 2002;124:3152–62.
33. Nivorozhkin AL et al. Enzyme-Activated Gd(3+) Magnetic Resonance Imaging Contrast Agents with a Prominent Receptor-Induced Magnetization Enhancement We thank Dr Shrikumar Nair for helpful discussions. Angew Chem. 2001;40:2903–6.
34. Makowski MR et al. Assessment of atherosclerotic plaque burden with an elastin-specific magnetic resonance contrast agent. Nat Med. 2011;17:383–8. doi:10.1038/nm.2310.
35.• Andia ME et al. Fibrin-targeted magnetic resonance imaging allows in vivo quantification of thrombus fibrin content and identifies thrombi amenable for thrombolysis. Arterioscler Thromb Vasc Biol. 2014;34:1193–8. doi:10.1161/ATVBAHA.113.302931. *This study demonstrates the use of in situ fibrin quantification as a readout marker for identifying amenable for thrombolysis.*
36. Flacke S et al. Novel MRI contrast agent for molecular imaging of fibrin: implications for detecting vulnerable plaques. Circulation. 2001;104:1280–5.
37. Winter PM et al. Molecular imaging of angiogenesis in early-stage atherosclerosis with alpha(v)beta3-integrin-targeted nanoparticles. Circulation. 2003;108:2270–4. doi:10.1161/01.CIR.0000093185.16083.95.
38. Weinmann HJ, Brasch RC, Press WR, Wesbey GE. Characteristics of gadolinium-DTPA complex: a potential NMR contrast agent. AJR Am J Roentgenol. 1984;142:619–24. doi:10.2214/ajr.142.3.619.
39. Laniado M, Weinmann HJ, Schorner W, Felix R, Speck U. First use of GdDTPA/dimeglumine in man. Physiol Chem Phys Med NMR. 1984;16:157–65.
40. Caravan P, Ellison JJ, McMurry TJ, Lauffer RB. Gadolinium(III) Chelates as MRI Contrast Agents: Structure, Dynamics, and Applications. Chem Rev. 1999;99:2293–352.
41. Weissleder R et al. Ultrasmall superparamagnetic iron oxide: characterization of a new class of contrast agents for MR imaging. Radiology. 1990;175:489–93. doi:10.1148/radiology.175.2.2326474.
42. Farrar CT et al. Impact of field strength and iron oxide nanoparticle concentration on the linearity and diagnostic accuracy of off-resonance imaging. NMR Biomed. 2008;21:453–63. doi:10.1002/nbm.1209.
43. Wang YX, Xuan S, Port M, Idee JM. Recent advances in superparamagnetic iron oxide nanoparticles for cellular imaging and targeted therapy research. Curr Pharm Des. 2013;19:6575–93.
44. Tang TY et al. Iron oxide particles for atheroma imaging. Arterioscler Thromb Vasc Biol. 2009;29:1001–8. doi:10.1161/ATVBAHA.108.165514.
45. Segers FM et al. Scavenger receptor-AI-targeted iron oxide nanoparticles for in vivo MRI detection of atherosclerotic lesions. Arterioscler Thromb Vasc Biol. 2013;33:1812–9. doi:10.1161/ATVBAHA. 112.300707.
46. Yilmaz A et al. Magnetic resonance imaging (MRI) of inflamed myocardium using iron oxide nanoparticles in patients with acute myocardial infarction - preliminary results. Int J Cardiol. 2013;163:175–82. doi:10.1016/j.ijcard.2011.06.004.
47. Islam T, Harisinghani MG. Overview of nanoparticle use in cancer imaging. Cancer Biomark : Sect Dis Markers. 2009;5:61–7. doi:10.3233/CBM-2009-0578.
48. Briley-Saebo KC, Mani V, Hyafil F, Cornily JC, Fayad ZA. Fractionated Feridex and positive contrast: in vivo MR imaging of atherosclerosis. Magnetic Reson Med : off J Soc Magn Reson Med / Soc Magn Reson Med. 2008;59:721–30. doi:10.1002/mrm.21541.
49. Amirbekian V et al. Detecting and assessing macrophages in vivo to evaluate atherosclerosis noninvasively using molecular MRI. Proc Natl Acad Sci U S A. 2007;104:961–6. doi:10.1073/pnas.0606281104.
50. Ruehm SG, Corot C, Vogt P, Kolb S, Debatin JF. Magnetic resonance imaging of atherosclerotic plaque with ultrasmall superparamagnetic particles of iron oxide in hyperlipidemic rabbits. Circulation. 2001;103:415–22.
51. Kooi ME et al. Accumulation of ultrasmall superparamagnetic particles of iron oxide in human atherosclerotic plaques can be detected by in vivo magnetic resonance imaging. Circulation. 2003;107:2453–8. doi:10.1161/01.CIR.0000068315.98705.CC.
52. Tang TY et al. Correlation of carotid atheromatous plaque inflammation using USPIO-enhanced MR imaging with degree of luminal stenosis. Stroke J Cereb Circ. 2008;39:2144–7. doi:10.1161/STROKEAHA.107.504753.
53. Hays AG et al. Noninvasive visualization of coronary artery endothelial function in healthy subjects and in patients with coronary artery disease. J Am Coll Cardiol. 2010;56:1657–65. doi:10.1016/j.jacc.2010.06.036.
54.• Phinikaridou A et al. Noninvasive magnetic resonance imaging evaluation of endothelial permeability in murine atherosclerosis using an albumin-binding contrast agent. Circulation. 2012;126:707–19. doi:10.1161/CIRCULATIONAHA.112.092098. *This study demonstrate the noninvasive assessment of endothelial permeability and function with the use of an albumin-binding magnetic resonance contrast agent and its possible application as a surrogate marker for the in vivo evaluation of interventions that aim to restore the endothelium.*
55. Phinikaridou A, Andia ME, Passacquale G, Ferro A, Botnar RM. Noninvasive MRI monitoring of the effect of interventions on endothelial permeability in murine atherosclerosis using an albumin-binding contrast agent. J Am Heart Assoc. 2013;2:e000402. doi:10.1161/JAHA.113.000402.
56. Lobbes MB et al. Atherosclerosis: contrast-enhanced MR imaging of vessel wall in rabbit model–comparison of gadofosveset and gadopentetate dimeglumine. Radiology. 2009;250:682–91. doi:10.1148/radiol.2503080875.
57. Pedersen SF et al. CMR assessment of endothelial damage and angiogenesis in porcine coronary arteries using gadofosveset. J Cardiovasc Magn Reson : Off J Soc Cardiovasc Magn Reson. 2011;13:10. doi:10.1186/1532-429X-13-10.
58. Lobbes MB et al. Gadofosveset-enhanced magnetic resonance imaging of human carotid atherosclerotic plaques: a proof-of-concept study. Investig Radiol. 2010;45:275–81. doi:10.1097/RLI.0b013e3181d5466b.
59. McAteer MA et al. Magnetic resonance imaging of endothelial adhesion molecules in mouse atherosclerosis using dual-targeted microparticles of iron oxide. Arterioscler Thromb Vasc Biol. 2008;28:77-–83. doi:10.1161/ATVBAHA.107.145466.
60. Nahrendorf M et al. Noninvasive vascular cell adhesion molecule-1 imaging identifies inflammatory activation of cells in atherosclerosis. Circulation. 2006;114:1504–11. doi:10.1161/CIRCULATIONAHA.106.646380.
61. Sluimer JC et al. Thin-walled microvessels in human coronary atherosclerotic plaques show incomplete endothelial junctions relevance of compromised structural integrity for intraplaque microvascular leakage. J Am Coll Cardiol. 2009;53:1517–27. doi:10.1016/j.jacc.2008.12.056.
62. Kolodgie FD et al. Elimination of neoangiogenesis for plaque stabilization: is there a role for local drug therapy? J Am Coll Cardiol. 2007;49:2093–101. doi:10.1016/j.jacc.2006.10.083.
63. Russell DA, Abbott CR, Gough MJ. Vascular endothelial growth factor is associated with histological instability of carotid plaques. Br J Surg. 2008;95:576–81. doi:10.1002/bjs.6100.
64. Virmani R et al. Atherosclerotic plaque progression and vulnerability to rupture: angiogenesis as a source of intraplaque

hemorrhage. Arterioscler Thromb Vasc Biol. 2005;25:2054–61. doi:10.1161/01.ATV.0000178991.71605.18.
65. Manduteanu I, Simionescu M. Inflammation in atherosclerosis: a cause or a result of vascular disorders? J Cell Mol Med. 2012;16:1978–90. doi:10.1111/j.1582-4934.2012.01552.
66. Purushothaman KR, Sanz J, Zias E, Fuster V, Moreno PR. Atherosclerosis neovascularization and imaging. Curr Mol Med. 2006;6:549–56.
67. Kerwin WS et al. Inflammation in carotid atherosclerotic plaque: a dynamic contrast-enhanced MR imaging study. Radiology. 2006;241:459–68. doi:10.1148/radiol.2412051336.
68. Jaffer FA, Libby P, Weissleder R. Molecular and cellular imaging of atherosclerosis: emerging applications. J Am Coll Cardiol. 2006;47:1328–38. doi:10.1016/j.jacc.2006.01.029.
69. Tait JF. Imaging of apoptosis. J Nucl Med Off Publ Soc Nucl Med. 2008;49:1573–6. doi:10.2967/jnumed.108.052803.
70. van Tilborg GA et al. Annexin A5-functionalized bimodal nanoparticles for MRI and fluorescence imaging of atherosclerotic plaques. Bioconjug Chem. 2010;21:1794–803. doi:10.1021/bc100091q.
71. Ye D et al. Bioorthogonal cyclization-mediated in situ self-assembly of small-molecule probes for imaging caspase activity in vivo. Nat Chem. 2014;6:519–26. doi:10.1038/nchem.1920.
72. Pello OM, Silvestre C, De Pizzol M, Andres V. A glimpse on the phenomenon of macrophage polarization during atherosclerosis. Immunobiology. 2011;216:1172–6. doi:10.1016/j.imbio.2011.05.010.
73. Durand E et al. Magnetic resonance imaging of ruptured plaques in the rabbit with ultrasmall superparamagnetic particles of iron oxide. J Vasc Res. 2007;44:119–28. doi:10.1159/000098484.
74. Morishige K et al. High-resolution magnetic resonance imaging enhanced with superparamagnetic nanoparticles measures macrophage burden in atherosclerosis. Circulation. 2010;122:1707–15. doi:10.1161/CIRCULATIONAHA.109.891804.
75. Schmitz SA et al. Superparamagnetic iron oxide-enhanced MRI of atherosclerotic plaques in Watanabe hereditable hyperlipidemic rabbits. Investig Radiol. 2000;35:460–71.
76. Sigovan M et al. Rapid-clearance iron nanoparticles for inflammation imaging of atherosclerotic plaque: initial experience in animal model. Radiology. 2009;252:401–9. doi:10.1148/radiol.2522081484.
77. Smith BR et al. Localization to atherosclerotic plaque and biodistribution of biochemically derivatized superparamagnetic iron oxide nanoparticles (SPIONs) contrast particles for magnetic resonance imaging (MRI). Biomed Microdevices. 2007;9:719–27. doi:10.1007/s10544-007-9081-3.
78. Makowski MR et al. Noninvasive assessment of atherosclerotic plaque progression in ApoE-/- mice using susceptibility gradient mapping. Circ Cardiovasc Imaging. 2011;4:295–303. doi:10.1161/CIRCIMAGING.110.957209.
79. Howarth SP et al. Utility of USPIO-enhanced MR imaging to identify inflammation and the fibrous cap: a comparison of symptomatic and asymptomatic individuals. Eur J Radiol. 2009;70:555–60. doi:10.1016/j.ejrad.2008.01.047.
80. Tang TY et al. Comparison of the inflammatory burden of truly asymptomatic carotid atheroma with atherosclerotic plaques contralateral to symptomatic carotid stenosis: an ultra small superparamagnetic iron oxide enhanced magnetic resonance study. J Neurol Neurosurg Psychiatry. 2007;78:1337–43. doi:10.1136/jnnp.2007.118901.
81. Trivedi RA et al. Identifying inflamed carotid plaques using in vivo USPIO-enhanced MR imaging to label plaque macrophages. Arterioscler Thromb Vasc Biol. 2006;26:1601–6. doi:10.1161/01.ATV.0000222920.59760.df.
82. Flogel U et al. In vivo monitoring of inflammation after cardiac and cerebral ischemia by fluorine magnetic resonance imaging. Circulation. 2008;118:140–8. doi:10.1161/CIRCULATIONAHA.107.737890.
83. Burnett JR. Lipids, lipoproteins, atherosclerosis and cardiovascular disease. Clin Biochem Rev / Aust Assoc Clin Biochem. 2004;25:2.
84. Sirol M et al. Lipid-rich atherosclerotic plaques detected by gadofluorine-enhanced in vivo magnetic resonance imaging. Circulation. 2004;109:2890–6. doi:10.1161/01.CIR.0000129310.17277.E7.
85. Chen W et al. Incorporation of an apoE-derived lipopeptide in high-density lipoprotein MRI contrast agents for enhanced imaging of macrophages in atherosclerosis. Contrast Media Mol Imaging. 2008;3:233–42. doi:10.1002/cmmi.257.
86. Katsuda S, Kaji T. Atherosclerosis and extracellular matrix. J Atheroscler Thromb. 2003;10:267–74.
87. von Bary C et al. MRI of coronary wall remodeling in a swine model of coronary injury using an elastin-binding contrast agent. Circ Cardiovasc Imaging. 2011;4:147–55. doi:10.1161/CIRCIMAGING.109.895607.
88. Makowski MR et al. Three-dimensional imaging of the aortic vessel wall using an elastin-specific magnetic resonance contrast agent. Investig Radiol. 2012;47:438–44. doi:10.1097/RLI.0b013e3182588263.
89.• Phinikaridou A et al. Vascular remodeling and plaque vulnerability in a rabbit model of atherosclerosis: comparison of delayed-enhancement MR imaging with an elastin-specific contrast agent and unenhanced black-blood MR imaging. Radiology. 2014;271:390–9. doi:10.1148/radiol.13130502. *This study demonstrates that the use of ESMA allows accurate classification of vascular remodelling, showing that positive remodelling is associated with high risk lesions.*
90. Motoyama S et al. Multislice computed tomographic characteristics of coronary lesions in acute coronary syndromes. J Am Coll Cardiol. 2007;50:319–26. doi:10.1016/j.jacc.2007.03.044.
91. Motoyama S et al. Computed tomographic angiography characteristics of atherosclerotic plaques subsequently resulting in acute coronary syndrome. J Am Coll Cardiol. 2009;54:49–57. doi:10.1016/j.jacc.2009.02.068.
92. Gough PJ, Gomez IG, Wille PT, Raines EW. Macrophage expression of active MMP-9 induces acute plaque disruption in apoE-deficient mice. J Clin Invest. 2006;116:59–69. doi:10.1172/JCI25074.
93. Lancelot E et al. Evaluation of matrix metalloproteinases in atherosclerosis using a novel noninvasive imaging approach. Arterioscler Thromb Vasc Biol. 2008;28:425–32. doi:10.1161/ATVBAHA.107.149666.
94. Hyafil F et al. Monitoring of arterial wall remodelling in atherosclerotic rabbits with a magnetic resonance imaging contrast agent binding to matrix metalloproteinases. Eur Heart J. 2011;32:1561–71. doi:10.1093/eurheartj/ehq413.
95. Nicholls SJ, Hazen SL. Myeloperoxidase and cardiovascular disease. Arterioscler Thromb Vasc Biol. 2005;25:1102–11. doi:10.1161/01.ATV.0000163262.83456.6d.
96. Ronald JA et al. Enzyme-sensitive magnetic resonance imaging targeting myeloperoxidase identifies active inflammation in experimental rabbit atherosclerotic plaques. Circulation. 2009;120:592–9. doi:10.1161/CIRCULATIONAHA.108.813998.
97. Ronald JA et al. Comparison of gadofluorine-M and Gd-DTPA for noninvasive staging of atherosclerotic plaque stability using MRI. Circ Cardiovasc Imaging. 2009;2:226–34. doi:10.1161/CIRCIMAGING.108.826826.
98. Tavora F, Cresswell N, Li L, Ripple M, Burke A. Immunolocalisation of fibrin in coronary atherosclerosis: implications for necrotic core development. Pathology. 2010;42:15–22. doi:10.3109/00313020903434348.

99. Falk E, Fernandez-Ortiz A. Role of thrombosis in atherosclerosis and its complications. Am J Cardiol. 1995;75:3B–11B.
100. Spuentrup E et al. MR imaging of thrombi using EP-2104R, a fibrin-specific contrast agent: initial results in patients. Eur Radiol. 2008;18:1995–2005. doi:10.1007/s00330-008-0965-2.
101. Vymazal J et al. Thrombus imaging with fibrin-specific gadolinium-based MR contrast agent EP-2104R: results of a phase II clinical study of feasibility. Investig Radiol. 2009;44:697–704. doi:10.1097/RLI.0b013e3181b092a7.
102. Botnar RM et al. In vivo molecular imaging of acute and subacute thrombosis using a fibrin-binding magnetic resonance imaging contrast agent. Circulation. 2004;109:2023–9. doi:10.1161/01.CIR.0000127034.50006.C0.
103.•• Noguchi T et al. High-intensity signals in coronary plaques on non contrast T1-weighted magnetic resonance imaging as a novel determinant of coronary events. J Am Coll Cardiol. 2014;63:989–99. doi:10.1016/j.jacc.2013.11.034. *This study determines whether coronary high-intensity plaques visualized noninvasive by noncontrast T1-weighted imaging are significantly associated with coronary events and may thus represent a novel predictive factor.*